JOURNAL OF THERMOPHYSICS AND HEAT TRANSFER
Vol. 23, No. 3, July–September 2009

Modeling Thermal Transport in Nanoparticle Composites

Arvind Pattamatta* and Cyrus K. Madnia†
University at Buffalo, State University of New York, Buffalo, New York 14260-4400

DOI: 10.2514/1.39505

In this paper, the heat transfer in three-dimensional nanoparticle composites is simulated using the Boltzmann transport equation for phonon intensity. Several semiconductor materials are considered, with the emphasis placed on Bi_2Te_3–Sb_2Te_3 nanoparticle composite, due to its high thermoelectric conversion efficiency at room temperature. A unit-cell approach is used to model the periodic distribution of nanoparticles in the host. Both cubic and noncubic nanoparticle composites are considered. The phonon properties are based upon the phonon dispersion model, and the interfaces are assumed to be diffusely transmitting and reflecting. The thermal conductivity of nanocomposites is found to exhibit the classical size effect and is also found to be dependent on the atomic percentage of the particle. The three-dimensional nanoparticles exhibit values of thermal conductivity similar to the lower-dimensional nanostructures such as the superlattice and nanowire. A detailed comparison of the thermal field with the classical Fourier model indicates significant underprediction by the Fourier model in regions of high temperature around the interface of the particle. The scattering interfacial area per unit volume is found to be a useful parameter for comparing the values of thermal conductivity in different types of nanocomposites.

Nomenclature

A	=	total interfacial area
A_s	=	scattering interfacial area
a	=	lattice constant
C	=	volumetric specific heat, J/m^3K
D_p	=	density of states per unit volume
f_p	=	phonon distribution function
$\hbar$	=	Planck's constant divided by 2π, 1.054×10^{-34} Js/phonon
I	=	phonon intensity, $Wm^{-2}sr^{-1}$
Kn	=	Knudsen number, Λ/L
k	=	thermal conductivity, W/mK
k_x	=	x-direction thermal conductivity, W/mK
k_z	=	z-direction thermal conductivity, W/mK
L	=	nanocomposite size, m
L_h	=	host size, m
L_p	=	particle size, m
L_x	=	particle length in the x direction, m
L_y	=	particle length in the y direction, m
L_z	=	particle length in the z direction, m
N_θ	=	number of discrete polar angular divisions
N_ϕ	=	number of discrete azimuthal angular divisions
$\mathbf{n}$	=	normal vector
Q	=	heat flow, W
q	=	heat flux, W/m^2
$\mathbf{r}$	=	position vector
S	=	Seebeck coefficient, μV/K
$\mathbf{s}$	=	phonon direction vector
T	=	absolute temperature, K
$\bar{T}$	=	average temperature, K
T_{ref}	=	reference temperature, K
t	=	time, s
V	=	volume of the unit cell
v	=	average phonon group velocity, m/s
w_θ	=	quadrature weight corresponding to the polar angle
w_ϕ	=	quadrature weight corresponding to the azimuthal angle
x, y, z	=	coordinates
x^*	=	nondimensional x coordinate, $x/L_{Bi_2Te_3}$
y^*	=	nondimensional y coordinate, $y/L_{Bi_2Te_3}$
z^*	=	nondimensional z coordinate, $z/L_{Bi_2Te_3}$
η	=	y-direction cosine
θ	=	polar angle, rad
Λ	=	phonon mean free path, m
μ	=	x-direction cosine
ξ	=	z-direction cosine
σ	=	electrical conductivity, S/m
τ	=	frequency-independent phonon relaxation time, s
ϕ	=	azimuthal angle, rad
ω	=	phonon frequency, Hz

Subscripts

b	=	boundary
eq	=	equilibrium
h	=	host (Ge, GaAs, Bi_2Te_3)
p	=	nanoparticle (Si, AlAs, Sb_2Te_3)
x	=	x coordinate
y	=	y coordinate
z	=	z coordinate

I. Introduction

THE efficiency of thermoelectric conversion for a material is measured by the nondimensional figure of merit (ZT), defined as $ZT = \sigma S^2 T/k$ [1]. During the last decade, advances have been made in increasing ZT using nanostructures [2,3]. This is achieved by reducing the phonon thermal conductivity more than the electrical conductivity. It is found that scattering of energy carriers at interfaces plays a key role in the reduction of thermal conductivity [4], thereby increasing ZT. Recently, Venkatasubramanian [3] has reported a ZT of 2.4 for Bi_2Te_3–Sb_2Te_3 superlattice. However, superlattice grown by thin-film deposition techniques may not be suitable for thermoelectric applications, due to its high manufacturing cost and difficulty in scaling up for large-scale applications. Nanoparticle composites can offer a more economical alternative to superlattice in the quest for high-ZT materials [5]. Similar to nanowire composites, the features that make nanoparticles attractive for thermoelectric application are the size effect and the effect of atomic percentage. In addition to these, nanoparticles offer greater choice in terms of their

Presented as Paper 4112 at the 40th AIAA Thermophysics Conference, Seattle, WA, 23–26 June 2008; received 1 July 2008; revision received 11 December 2008; accepted for publication 8 February 2009.

*Graduate Student, Department of Mechanical and Aerospace Engineering. Student Member AIAA.

†Professor, Department of Mechanical and Aerospace Engineering. Associate Fellow AIAA.

shape and their distribution in the host material. These remarkable features of nanoparticle composites can be used to tailor the mechanical, thermal, electrical, and chemical properties that are best suited for a particular application.

Although nanoparticle composites seem to be promising for improving the thermoelectric efficiency, very little experimental or modeling work exist on characterizing energy transport in these materials. Because the characteristic dimensions of the nanostructures are often smaller than the mean free path of phonons, the conventional Fourier law of heat conduction is no longer valid [6]. Hence, a more rigorous modeling approach employing the Boltzmann transport equation (BTE) has to be used to describe the thermal characteristics of nanoparticles. The previous study on thermal transport in nanoparticles involved Monte Carlo simulation of the BTE, in which the phonons are modeled in a stochastic framework [7]. However, in stochastic simulations, it is more difficult to prescribe accurate boundary and interface conditions. Also, an extension to incorporate wave effects for ultrasmall sizes is not possible with particle-tracking methods.

The main objective of the present work is to extend the general deterministic framework of thermal modeling of 2-D nanowire composites [8,9] to simulate heat transport in 3-D nanoparticle composites using the BTE. The effects of particle size and the atomic percentage on the cubic Bi_2Te_3–Sb_2Te_3 nanoparticles are studied and compared with Ge–Si and GaAs–AlAs nanoparticles. The effect of nanoparticle shape on thermal transport is also studied for noncubic configurations. Comparisons between the results of BTE and the Fourier model are made to understand the deficiency of the phenomenological model.

II. Problem Description and Modeling

The schematic of the nanoparticle composite chosen for the present simulations and the 3-D coordinate system used in the simulations are shown in Fig. 1. The nanoparticle composite consists of either cubic or noncubic nanoparticles uniformly dispersed in a cubic host, as shown in Fig. 1a. Although, in practice, these nanoparticles may be randomly distributed in the host, the uniform distribution considered here offers computational simplicity. The materials considered for the host are bismuth telluride (Bi_2Te_3), germanium (Ge), and gallium arsenide (GaAs), and the corresponding materials for particles are antimony telluride (Sb_2Te_3), silicon (Si), and aluminum arsenide (AlAs). The nanoparticles are assumed to be uniformly distributed inside the host material. The heat is applied along the x and z directions. The 2-D unit-cell approach [10] is extended to 3-D, as shown in Fig. 1b, to simulate the effect of a single particle and the surrounding host material within the cell.

To investigate the heat transfer in nanocomposites, the main energy carriers in semiconductors (namely, phonons) are modeled via the Boltzmann transport equation for the phonon intensity in the relaxation-time approximation. The intensity of phonon radiation, I, is defined as the flux of energy per unit time, per unit area, and per unit solid angle in the direction $\mathbf{s}$ and is related to the phonon distribution function $f_p(\mathbf{r}, \mathbf{s}, t)$ as [11]

$$I(\mathbf{r}, \mathbf{s}, t) = \frac{1}{4\pi} \sum \int \hbar \omega v_p f_p(\mathbf{r}, \mathbf{s}, t) D_p(\omega) \mathrm{d}\omega \tag{1}$$

where $\mathbf{r}$ denotes the phonon position vector, $\hbar$ is Planck's constant divided by 2π, ω is the phonon frequency, v_p is the phonon velocity corresponding to each polarization mode, and $D_p(\omega)$ is the density of states per unit volume. The equilibrium distribution of phonons at temperature T is represented by the Bose–Einstein distribution [11].

Using the coordinate system shown in Fig. 1c, the frequency-independent BTE can be expressed as [12]

$$\frac{\partial I}{\partial t} + v\left(\mu \frac{\partial I}{\partial x} + \eta \frac{\partial I}{\partial y} + \xi \frac{\partial I}{\partial z}\right) = \frac{I_{\mathrm{eq}} - I}{\tau} \tag{2}$$

where

$$I_{\mathrm{eq}} = \frac{1}{4\pi} \int_0^{2\pi} \int_{-1}^{1} I \mathrm{d}\mu \mathrm{d}\phi$$

where μ, η, and ξ are the x, y, and z direction cosines, respectively, and v is the average phonon group velocity. The solution to BTE requires knowledge of the phonon relaxation time, group velocity, and specific heat. A frequency-independent relaxation-time approach, also referred to as the *phonon gray medium approximation*, is used in the present simulations. The effective relaxation time τ is calculated from the phonon mean free path Λ and average group velocity v as $\tau = \Lambda / v$. The material properties used in the computation are evaluated using the phonon sine-function dispersion model proposed by Chen [13]. This model uses the frequency-averaged specific heat and velocity to calculate the phonon mean free path and gives a more accurate estimate of the material properties, compared with the conventional Debye model [8]. Table 1 summarizes the properties of Ge, Si, GaAs, AlAs, Bi_2Te_3, and Sb_2Te_3 calculated using the dispersion model at 300 K.

The BTE for the phonon intensity is solved in conjunction with suitable boundary and interface treatments. The treatment of interfaces between the two materials significantly affects the thermal characteristics of the nanocomposite. Ziman [14] proposed the following expression for estimating the interface specularity parameter p:

$$p = \exp\left(-\frac{16\pi^3 \delta^2}{\lambda^2}\right) \tag{3}$$

where δ is the interface roughness and λ is the phonon wavelength. Recently, Zhang [15] presented this expression with a π^2 dependence, rather than the widely quoted π^3 dependence shown in Eq. (3). A value of p equal to zero indicates a totally diffuse interface, and a value equal to one indicates a totally specular interface. At room temperature, the characteristic phonon wavelengths for the materials considered are approximately 8–9 Å. Even if one-monolayer roughness, $\delta = 4$ Å, is considered, this expression gives an interface specularity parameter $p \sim 0$, which shows that the interfaces scatter diffusely. Hence, in the present case, the interfaces are treated as totally diffusive, and the diffuse mismatch model (DMM) [16] is used. This model makes an assumption that the

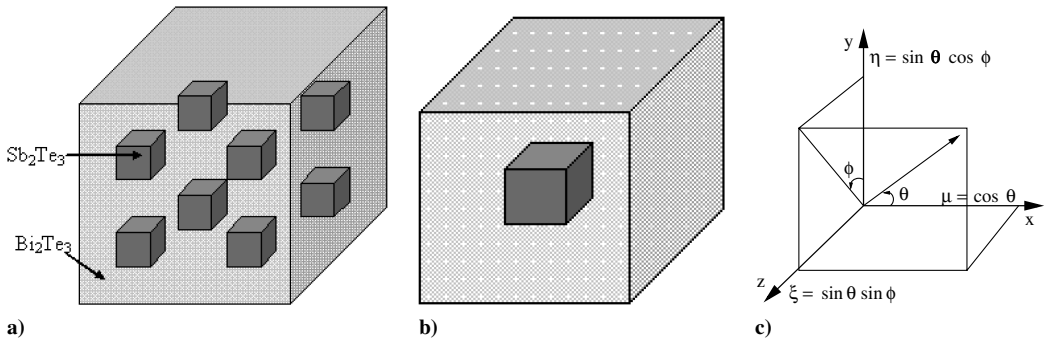

Fig. 1 Schematic of a) nanoparticle composite, b) unit cell, and c) 3-D coordinate system.

Table 1 Material properties calculated using phonon sine-function dispersion model

Material	k, W/mK	C $\times 10^6$, J/m^{3}K	v, m/s	Λ, Å
Ge	60	0.87	1042	1986
Si	145.6	0.93	1804	2604
GaAs	43.6	0.88	1024	1453
AlAs	86.4	0.88	1246	2364
Bi_2Te_3	1.1	0.5	212	310
Sb_2Te_3	0.9	0.53	200	254

phonons emerging from an interface are independent of the phonons incident on the interface.

The top and the bottom boundaries of the unit cell are treated as adiabatic surfaces and the remaining boundaries are modeled as periodic, to maintain continuity of heat flow [8]. The adiabatic condition is modeled as a specularly reflecting boundary on which the following condition for intensity is imposed:

$$I(\mathbf{r}_b, \mathbf{s}, t) = I(\mathbf{r}_b, \mathbf{s}_r, t) \tag{4}$$

where $\mathbf{s}_r = \mathbf{s} - 2(\mathbf{s} \cdot \mathbf{n})\mathbf{n}$, $\mathbf{n}$ is the outward normal vector, and $\mathbf{r}_b$ denotes the spatial coordinates of the boundary.

III. Numerical Methodology

The first-order upwind scheme is used for the spatial discretization of the BTE. An explicit Euler time-stepping method is used for temporal discretization, to allow the solution to reach a steady state. The angular discretization is performed through the decomposition of the polar and azimuthal angles into discrete directions such that $0 \le \theta \le \pi$ and $0 \le \phi \le 2\pi$ are discretized into N_θ and N_ϕ angular points, respectively. All angular integrations are performed using Gauss–Legendre quadratures, which discretizes the polar and azimuthal angles and assigns suitable weights for each direction [17]. It has been shown that the use of Gauss–Legendre quadrature successfully resolves the ray-effect problem encountered in phonon radiative transport [18].

To accurately capture the temperature jumps across the interfaces of the two materials, a nonuniform grid with a suitable compression is used at all the interfaces. A detailed spatial and angular grid resolution study is performed to test for grid independence of the solution. It is found that a spatial grid with $128 \times 128 \times 128$ points and an angular decomposition with 30×20 points provide the best resolution of the thermal field. A temporal resolution study has also been performed to determine the time step that ensures accurate transient solution.

The numerical solution to the BTE is computationally prohibitive on a single processor, due to an excessive grid size of $128 \times 128 \times 128 \times 30 \times 20$. Hence, the code has been parallelized in the x and y directions using message-passing interface communication routines [19], and the parallel efficiency study indicates a near-linear scaleup from 2 to 128 processors. The parallel computations incur a CPU time per iteration of 65 s using 128 processors.

IV. Results and Discussion

The parameters that have been varied to study their effect on the thermal characteristics of the nanoparticle composite are the particle size, atomic percentage (AP), and the particle aspect ratio (AR). The atomic percentage of the nanoparticle is related to the volumetric percentage (VP) and the lattice constant a as [8]

$$\mathrm{AP} = \frac{\mathrm{VP}}{(\mathrm{VP} + (1 - \mathrm{VP})(a_p/a_h))} \tag{5}$$

For the cubic nanoparticle composite, $\mathrm{VP} = L_p^3/L_h^3$, where L_p and L_h are the lengths of the particle and host, respectively. AR is defined as the ratio of nanoparticle length in the z direction to its length in the x direction: L_z/L_x.

The phonon intensity obtained from solving the BTE is then used to determine the heat flux, temperature distribution, and thermal conductivities. At nanoscales, the temperature, as such, has no physical meaning except that it is an indicator of the local energy density of the system. The effective temperature is obtained from phonon intensity as

$$T(x, y, z) = \frac{1}{C_h v_h} \sum_{N_\theta} \sum_{N_\phi} I(x, y, z, \theta, \phi) w_\theta w_\phi \tag{6}$$

where w_θ and w_ϕ are the weights associated with the polar and azimuthal directions, respectively. The heat fluxes in the x and z directions (namely, q_x and q_z) are related to the intensity through the relations

$$q_x(x, y, z) = \sum_{N_\theta} \sum_{N_\phi} I(x, y, z, \theta, \phi) \mu w_\theta w_\phi \tag{7}$$

$$q_z(x, y, z) = \sum_{N_\theta} \sum_{N_\phi} I(x, y, z, \theta, \phi) \xi w_\theta w_\phi \tag{8}$$

For the noncubic nanoparticle composite, the effective thermal conductivities in the x direction, k_x, and in the z direction, k_z, can be defined as

$$k_x = \frac{Q_x L_x}{L_y L_z (\bar{T}(x = 0) - \bar{T}(x = L_h))}; \qquad k_z = \frac{Q_z L_z}{L_x L_y (\bar{T}(z = 0) - \bar{T}(z = L_h))} \tag{9}$$

where Q_x and Q_z are the heat flow in the x and z directions, respectively. $\bar{T}$ is the area-averaged temperature at the boundary. For the cubic nanoparticle composite, $k = k_x = k_y$, due to symmetries in geometry and heat flow for all three coordinate directions.

A. Validation of the BTE Solver

To validate the three-dimensional BTE solver, two cases are considered. First, the 3-D steady-state heat transfer in Ge–Si nanowire composite is examined, and the resulting thermal conductivity along the wire axis, k_z, is compared with the analytical solution of Prasher [20]. In the BTE simulations, the nanowires have a square cross section of the same equivalent diameter as the cylindrical wires used in the analytical study. Figure 2a shows the effect of the volumetric percentage on thermal conductivity for different wire sizes ranging from 20 to 1000 nm. The predicted thermal conductivity is found to be in good agreement with the analytical solution for different wire sizes. For the smallest wire size of 20 nm, the thermal conductivity decreases with increasing volumetric percentage, due to the increase in the scattering of phonons from the Ge–Si interfaces. However, for a wire size of 1000 nm, the thermal conductivity of the nanocomposite increases with volumetric percentage of Si. This is due to the material properties of Ge–Si nanocomposite, in which the bulk thermal conductivity of Si equal to 145 W/mK is higher than that of Ge, which is equal to 60 W/mK. The second validation case involves comparison of BTE results for thermal conductivity of Ge–Si nanoparticle composite with the results of Monte Carlo (MC) simulation by Jeng et al [7]. Figure 2b shows the effect of atomic percentage on thermal conductivity of nanoparticle composites for both BTE and MC simulations. For all three particle sizes of 10, 50, and 200 nm, k shows a decreasing trend with increasing atomic percentage of Si. The thermal conductivity predicted from our simulation is in good agreement with the MC simulations. These results highlight the capability of our 3-D code used to solve for energy transport in nanoparticle composites. The BTE code is thus applied to simulate phonon transport in both cubic and noncubic nanoparticle composite configurations.

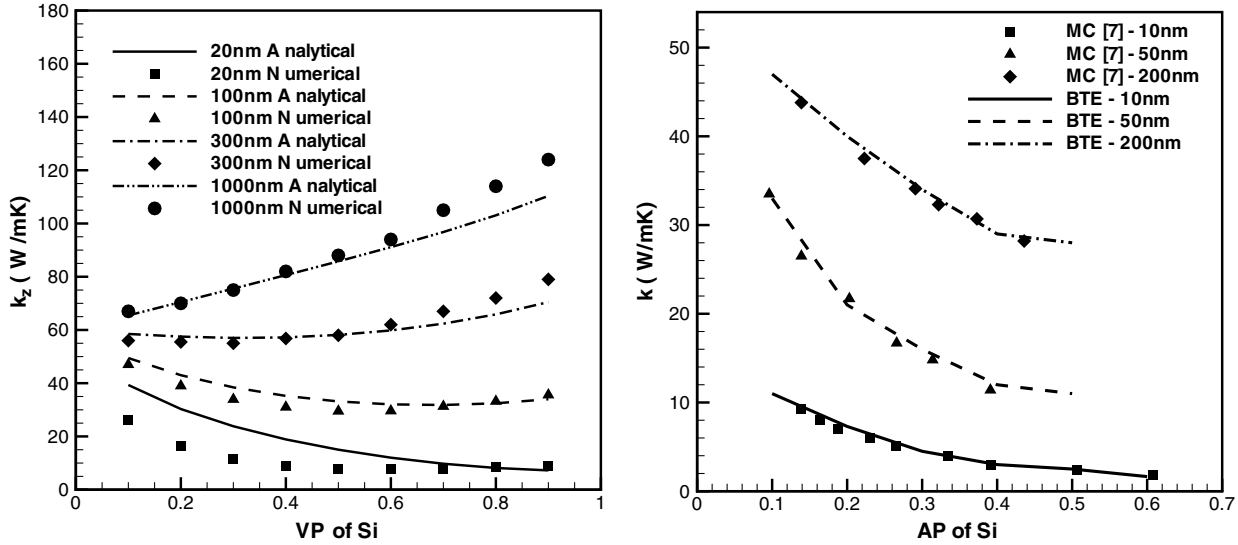

a) b)

Fig. 2 Plots of a) axial thermal conductivity of 3-D Ge–Si nanowire and b) variation of the thermal conductivity of Ge–Si nanoparticle with atomic percentage of Si.

B. Thermal Characteristics of Cubic Nanoparticle Composites

The steady-state heat transport simulations are performed for the cubic Sb_2Te_3 nanoparticle suspended in Bi_2Te_3 host material. The nature of phonon transport is characterized by a nondimensional ratio of phonon mean free path to the particle size, called the Knudsen number Kn. $Kn \gg 1$ indicates ballistic limit and $Kn \ll 1$ indicates the Fourier limit. Figure 3a shows $T - T_{\text{ref}}$ temperature contours for a Knudsen number of 10 with heat transport in both the x and z directions. The reference temperature $T_{\text{ref}} = 300$ K. The same temperature difference is applied in both directions, leading to a heat flux ratio q_x/q_z of 1. The temperature contours show nonlinearity in the temperature distribution both inside the particle and in the host, due to significant phonon scattering at the interfaces between the two materials. The contours are clustered near the interfaces, where the interface scattering dominates the interior scattering of phonons.

To better understand the effects of scattering from the particle interfaces, the temperature profiles are shown at two different y locations, as seen in Fig. 3b. In the x–y plane, these are at midway, $y^* = 0.5$, and through the top interface at $y^* = 0.79$. The temperature jumps occurring at the interface between the host and the particle can be attributed to interface thermal resistance, which has also been observed for the superlattice and nanowire composites [8,18]. To compare the effect of the Knudsen number on the temperature, its profile for the ballistic case of $Kn = 10$ is compared with the transitional ($Kn = 1$) and Fourier ($Kn = 0.1$) cases. For the case of $Kn = 10$, the left interface has a higher temperature, and the right interface has a lower temperature than the boundary temperatures, resulting in a change in the sign of temperature gradient along the x direction. Similar results were obtained by Yang and Chen [18] and by Pattamatta and Madnia [8] in the ballistic limit for Ge–Si and Bi_2Te_3–Sb_2Te_3 nanowire composites, respectively. However, this is not observed for the lower-Knudsen-number cases, in which ballistic effects are less pronounced. The temperature profiles in the y–z plane corresponding to heat flow in the z direction also show a

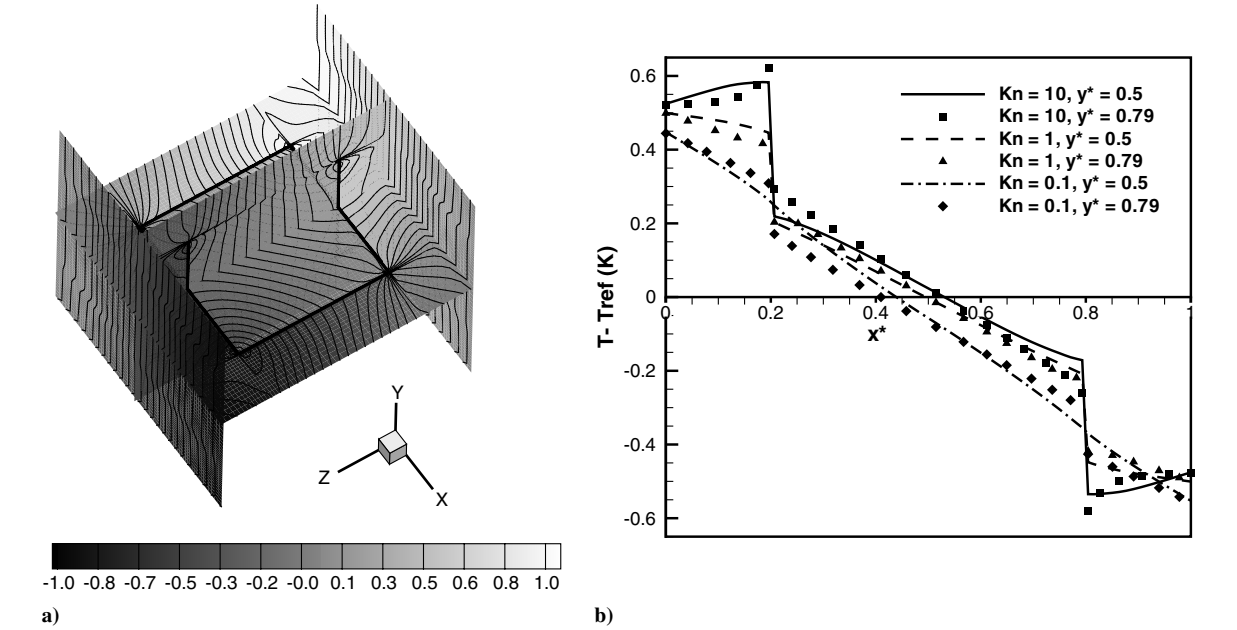

a) b)

Fig. 3 Plots of a) temperature contours for Bi_2Te_3–Sb_2Te_3 nanoparticle composite for AP = 0.2 and $L_{Sb_2Te_3} = 25.4$ Å and b) temperature profiles ($T - T_{\text{ref}}$) for AP = 0.2.

similar trend to that in the x direction, due to the cubic nature of the nanoparticle and due to uniform heat fluxes in both of these directions.

The variation of effective thermal conductivity k of the cubic Bi_2Te_3–Sb_2Te_3 nanoparticle composite with the particle size for atomic percentages of 0.2 and 0.8 is shown in Fig. 4a. As a reference, the thermal conductivities for Bi_2Te_3–Sb_2Te_3 superlattice and Bi_2Te_3–Sb_2Te_3 nanowire are also shown on the this figure. The thermal conductivity decreases with decreasing particle size. This is attributed to the increase in phonon scattering at the interfaces of the nanoparticle, due to ballistic effects with decreasing particle size [18]. The dependence of thermal conductivity on particle size is called the *classical size effect*. For AP = 0.2, the values of thermal conductivity of the cubic nanoparticle composite are close to those of superlattice and nanowire composites. For larger sizes, the thermal conductivities of the nanoparticle, nanowire, and superlattice composites approach their respective bulk values, the bulk value of nanoparticle composite being higher than the nanowire and superlattice composites. However, for the case of AP = 0.8, for larger particle sizes, the thermal conductivity of the nanoparticle composite is lower than the nanowire and superlattice composites. For particle sizes less than 25 Å, the phonon wavelength of 9 Å becomes comparable with the dimension of the nanoparticle and wave effects may need to be considered. The wave effects were observed in the experiment of Venkatasubramanian [21] for Bi_2Te_3–Sb_2Te_3 superlattice, when the superlattice period thickness was smaller than 25 Å. Figure 4a also shows that for a given particle size, the thermal conductivity corresponding to AP = 0.8 is lower than that of AP = 0.2, due to an increase in ballistic effects in the host for AP = 0.8.

Figure 4b shows the effect of atomic percentage on the thermal conductivity of Bi_2Te_3–Sb_2Te_3, Ge–Si, and GaAs–AlAs nanocomposites. The atomic percentage is varied from 0.1 to 0.9, keeping the particle Knudsen number fixed at 10. For a given particle size, increasing the atomic percentage results in a decrease in the size of the host. This results in higher phonon interface scattering and hence a decrease of thermal conductivity. The thermal conductivity values for the Bi_2Te_3–Sb_2Te_3 nanoparticle composite is similar to the superlattice and nanowire composites. The Ge–Si and GaAs–AlAs nanoparticle composites show similar atomic percentage effects, but their thermal conductivities are approximately 2 orders of magnitude higher than that of Bi_2Te_3–Sb_2Te_3. This highlights the importance of using Bi_2Te_3–Sb_2Te_3 nanostructures for efficient thermoelectric applications.

C. Thermal Characteristics of Noncubic Nanoparticle Composites

Noncubic nanoparticle composites can be used to effectively control the thermoelectric properties in different directions of the nanocomposite. The effective thermal conductivity for these nanocomposites is nonisotropic and is a function of the direction of heat transport. In this section, the effect of a varying AR of the nanoparticle on the temperature profiles and thermal conductivity is studied. The nanoparticle is assumed to have a square cross section such that $L_x = L_y$ in the x–y plane. For a given atomic percentage, the value of the aspect ratio is limited, above which the particle length L_z becomes larger than the size of the host. For AP of 0.2 and 0.8, the maximum AR approaches 2 and 1.1, respectively.

Figure 5a shows the effect of varying the aspect ratio on temperature profiles of Bi_2Te_3–Sb_2Te_3 nanoparticle composite. The profiles are plotted as a function of the location along the z axis at $y^* = 0.5$. It is observed that for a fixed atomic percentage, increasing the aspect ratio moves the location of the peak temperature jumps closer to the boundaries of the host. Also, the temperature jumps are smaller at the interfaces for higher-aspect-ratio nanoparticles. Figure 5b shows the effect of aspect ratio on k_x and k_z for atomic percentages of 0.2 and 0.8. The abscissa on the bottom and the ordinate on the left side of the figure correspond to an AP of 0.2, and the top abscissa and ordinate on the right side correspond to an AP of 0.8. For both atomic percentages, k_x decreases, whereas k_z increases with increasing aspect ratio. This can be attributed to an increase in phonon interfacial scattering in the y–z plane. By increasing the aspect ratio of the nanoparticle, k_x is found to reduce by 23 and 30%, corresponding to the atomic percentages of 0.2 and 0.8, respectively.

Figure 6 shows the effect of particle size and atomic percentage on the thermal conductivities for the highest aspect ratios. From Fig. 6a, it is seen that for very small particle sizes, corresponding to the ballistic limit, the values of k_x and k_z are close to the thermal conductivity of the cubic nanoparticle composite. With increasing particle size, k_x is lower and k_z is higher than the thermal conductivity of the cubic nanoparticle composite. The thermal conductivity value for the Bi_2Te_3–Sb_2Te_3 nanoparticle composite corresponding to AP = 0.8 is lower than that of AP = 0.2. Figure 6b shows the effect of atomic percentage on thermal conductivity for different nanoparticle composite materials. Similar to that of the cubic nanoparticle composite, k_x and k_z for the noncubic nanoparticle composite also decrease with increasing atomic percentage. The relative difference between the thermal conductivity values for the cubic and noncubic Bi_2Te_3–Sb_2Te_3 nanoparticle composites is larger than the Ge–Si and GaAs–AlAs nanocomposites.

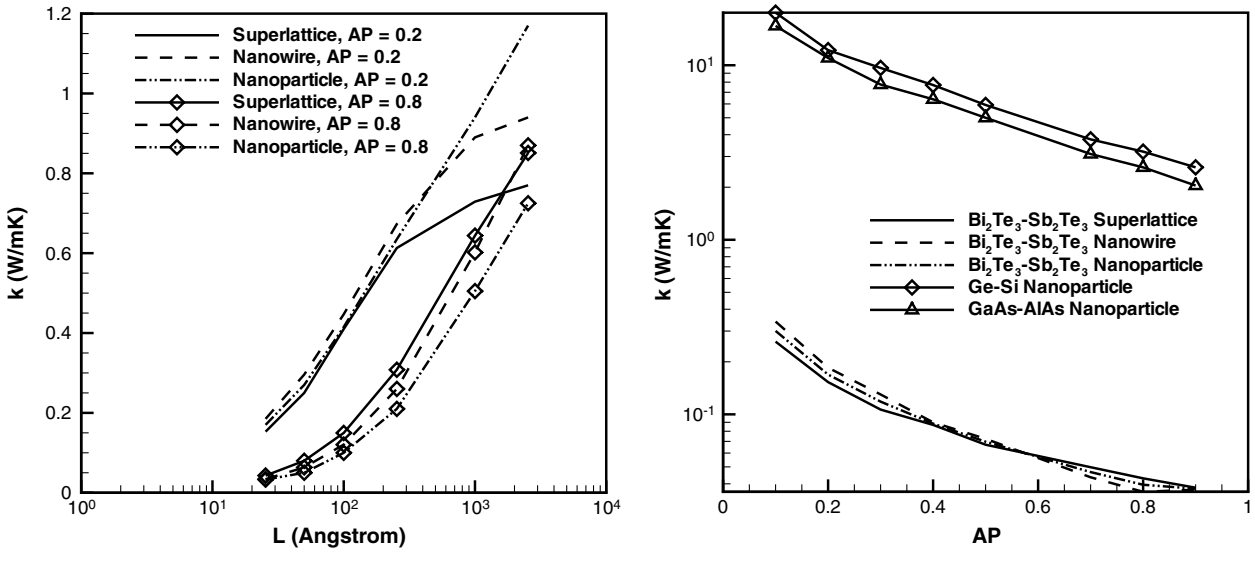

Fig. 4 Plots of a) size effect on thermal conductivity of Bi_2Te_3–Sb_2Te_3 nanocomposites. b) effect of atomic percentage on thermal conductivity of nanostructures for $Kn = 10$.

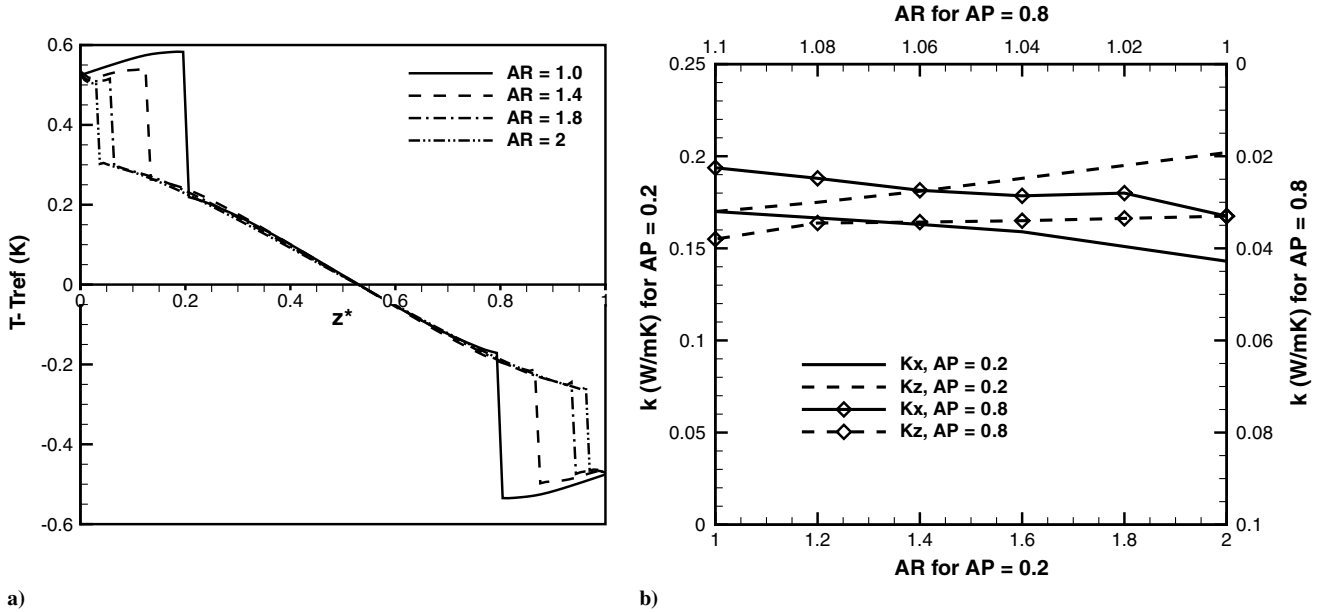

a) b)

Fig. 5 Plots of a) variation of temperature with the aspect ratio of noncubic Bi_2Te_3–Sb_2Te_3 nanoparticle composite for AP = 0.2 and b) effect of aspect ratio on the thermal conductivity for $L_{Sb_2Te_3} = 25.4$ Å and for AP = 0.2 and 0.8.

To highlight the limitations of the classical Fourier model when applied to heat transport in nanoparticle composites, comparison is made between the BTE and Fourier results shown in Fig. 7. Figures 7a and 7c show the relative percentage differences between the BTE and Fourier temperature prediction for the Bi_2Te_3–Sb_2Te_3 noncubic nanoparticle composite plotted in the x–y and x–z planes, respectively. The relative percentage difference is expressed as $(T_{BTE} - T_{Fourier}) \times 100/T_{BTE}$. The positive values indicate underprediction by the Fourier model. The regions near the interface of the two materials, where the maxima and minima in the temperatures occur, show the maximum differences between the two models. The Fourier model underpredicts regions of maximum temperature by as much as 50% and overpredicts the regions of minimum temperature by 30%. This is consistent with the results of nanoscale silicon on insulator, in which the regions of peak phonon temperatures or hot spots are significantly underestimated in the Fourier solution [22]. Figures 7b and 7d show the percentage difference in x-direction heat fluxes between the BTE and Fourier models for the two planes. The Fourier model underestimates the heat flux throughout the nanocomposite by as much as 100%. In the x–y plane, the percentage difference varies between 85 to 100%, whereas in the x–z plane, it varies between 70 to 100%.

The thermal conductivity of the Bi_2Te_3–Sb_2Te_3 nanoparticle composites for different cases are plotted as a function of the total interfacial area per unit volume, A/V, and scattering interfacial area per unit volume, A_s/V, in Figs. 8a and 8b, respectively. Table 2 describes the cases for Bi_2Te_3–Sb_2Te_3 nanocomposites shown in Fig. 8.

The cases shown include the effect of atomic percentage for $Kn = 10$ and size effect for AP = 0.2 and 0.8. Figure 8 shows a better collapse of the thermal conductivity data plotted as a function of the scattering interfacial area per unit volume as compared with the total interfacial area per unit volume. This can be attributed to the fact that the cross-sectional area normal to heat flow is the main contributor to phonon scattering and change in thermal conductivity. A power-law fit through the data in Fig. 8a follows the relationship

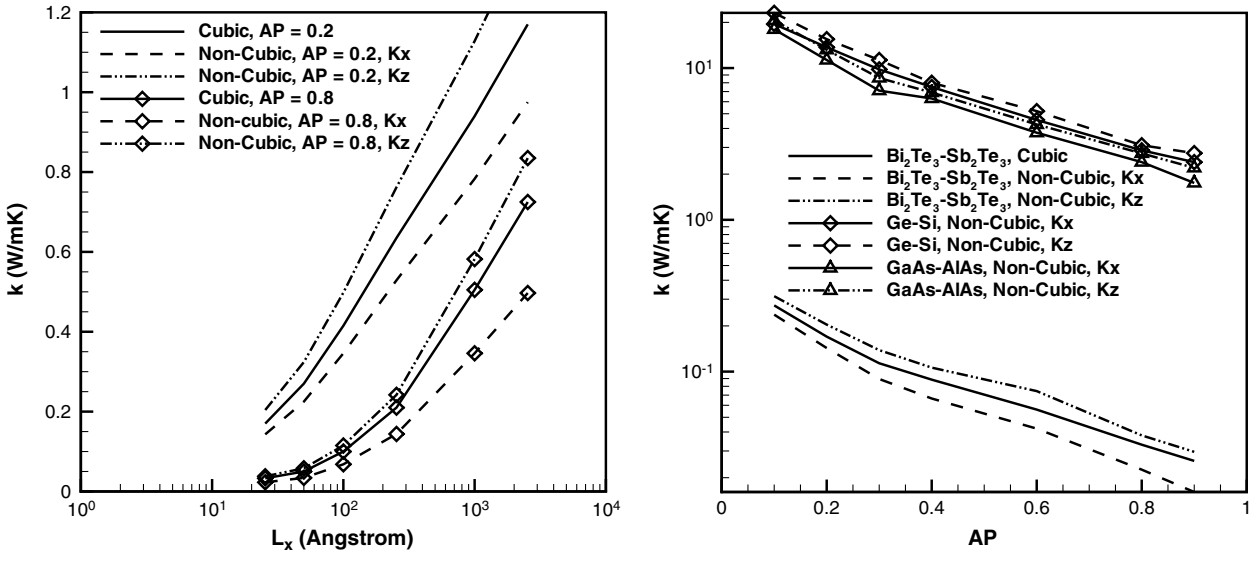

a) b)

Fig. 6 Plots of a) size effect on thermal conductivity of noncubic Bi_2Te_3–Sb_2Te_3 nanoparticle composite and b) effect of atomic percentage on thermal conductivity of noncubic nanoparticle composites for $Kn = 10$.

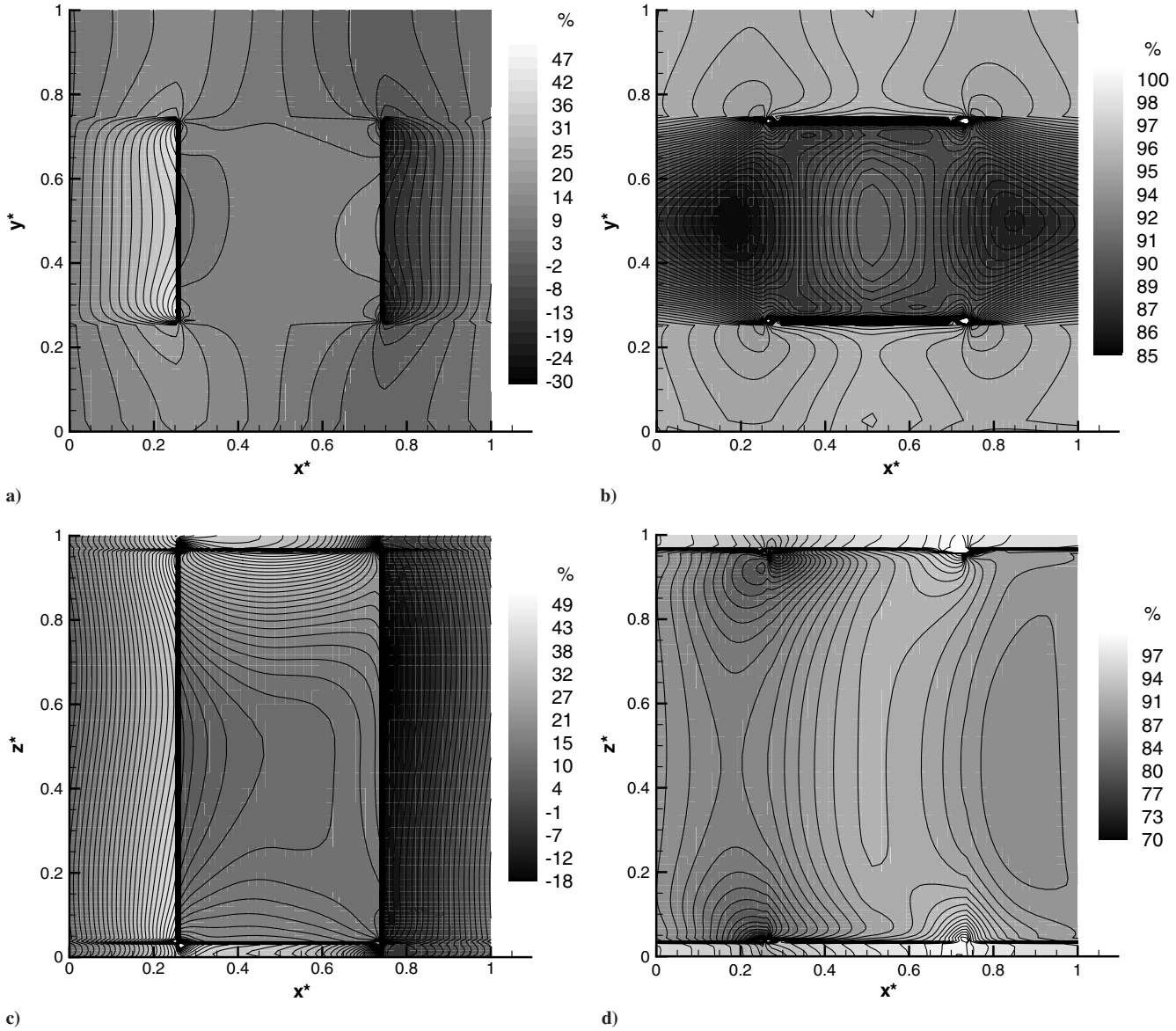

Fig. 7 Percentage difference between BTE and Fourier simulations as observed in temperature contours (left) and heat flux contours (right) for a noncubic Bi_2Te_3–Sb_2Te_3 nanoparticle composite for $Kn = 10$, AP = 0.2, and AR = 2.

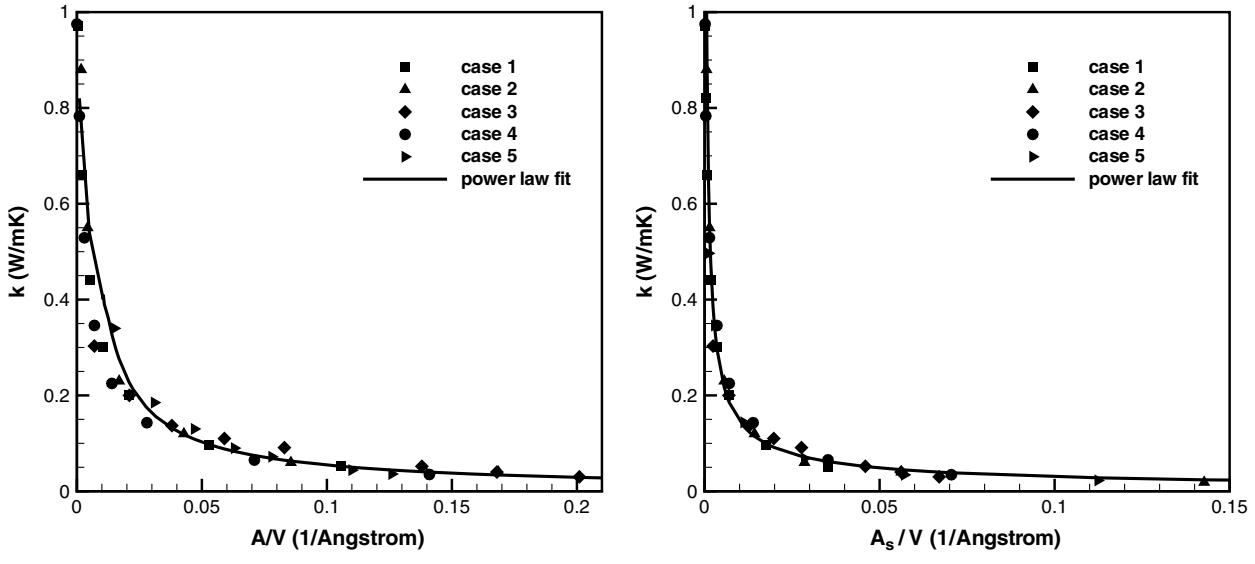

Fig. 8 Thermal conductivity as a function of a) total interface area per unit volume b) scattering interface area per unit volume for Bi_2Te_3–Sb_2Te_3 nanoparticles.

Table 2 Description of cases for Bi_2Te_3–Sb_2Te_3 nanoparticle composites plotted in Fig. 8

Case	Configuration	Kn	AP
1	Nanoparticle, cubic	0.1–10	0.2
2	Nanoparticle, cubic	0.1–10	0.8
3	Nanoparticle, cubic	10	0.1–0.9
4	Nanoparticle, noncubic	0.1–10	0.2
5	Nanoparticle, noncubic	0.1–10	0.8

$k = 0.0067(A/V)^{-0.911}$ and in Fig. 8b follows the relationship $k = 0.0063(A_s/V)^{-0.6824}$.

V. Conclusions

The heat transfer across nanoparticle composites is studied by solving the 3-D Boltzmann transport equation (BTE) for phonon intensity in the relaxation-time approximation. Emphasis is placed upon the Bi_2Te_3–Sb_2Te_3 nanoparticle composite configuration, due to its relative importance for room-temperature thermoelectric applications. The BTE results are compared with the existing analytical solution for Ge–Si nanowire composite and with the Monte Carlo simulation for Ge–Si nanoparticle composite. Both cubic and noncubic Bi_2Te_3–Sb_2Te_3 nanoparticle composites are modeled and compared with the Ge–Si and GaAs–AlAs nanocomposites. The phonon mean free path, group velocity, and specific heat are calculated from the phonon sine-function dispersion model. A 3-D unit cell is selected with periodic boundaries, and the interfaces are treated as totally diffusive using the DMM. The resulting temperature profiles in the ballistic limit show jumps at the interfaces due to interface thermal resistance. This leads to a decrease in thermal conductivity with a decrease in size and an increase in atomic percentage of the particle. The temperature profiles in the z direction for the noncubic nanoparticle composites show decreasing interfacial jumps with increasing aspect ratio of the nanoparticle. The thermal conductivity of the cubic nanoparticle composite exhibits significant size effect and atomic percentage dependency that are comparable with the superlattice and nanowire composite configurations. In addition, the noncubic nanoparticle composite shows directional dependency of thermal conductivity, wherein the thermal conductivity along the x direction, k_x, is reduced below the value of a cubic nanoparticle composite. This directionality in thermal conductivity can help in tailoring thermoelectric properties. A comparison of the BTE solution is made with the solution of heat conduction using Fourier's law. The Fourier solution is found to have significant deviation by as much as 50% in the temperature-profile prediction. The heat flux is underpredicted by Fourier law by up to 100% near the boundaries of the nanoparticle composite. The scattering interfacial area per unit volume is found to be a useful parameter for comparing the values of thermal conductivity in different types of nanocomposites.

Acknowledgments

We acknowledge funding support from the Donors of the Petroleum Research Funds administered by the American Chemical Society under grant no. 41643-AC9. The computational resources were provided by the Center for Computational Research (CCR) at the University at Buffalo, State University of New York and by the National Center for Supercomputing Research (NCSA) under CTS030034N.

References

[1] Goldsmid, H. J., *Thermoelectric Refrigeration*, Plenum, New York, 1964.

[2] Dresselhaus, M. S., Chen, G., Tang, M. Y., Yang, R., Lee, H., Wang, D., Ren, Z., Fleurial, J., and Gogna, P., "New Directions for Low-Dimensional Thermoelectric Materials," *Advanced Materials*, Vol. 19, No. 8, 2007, p. 1.

[3] Venkatasubramanian, R., Colpitts, E. S. T., and O'Quinn, B., "Thin-Film Thermoelectric Devices with High Room-Temperature Figures of Merit," *Nature*, Vol. 413, No. 6856, 2001, pp. 597–602. doi:10.1038/35098012

[4] Chen, G., "Thermal Conductivity and Ballistic Transport In the Cross Plane Direction of Superlattices," *Physical Review B*, Vol. 57, No. 23, 1998, pp. 14958–14973. doi:10.1103/PhysRevB.57.14958

[5] Chen, G., "Nanoscale Heat Transfer and Nanostructured Thermoelectrics," *IEEE Transactions on Components and Packaging Technologies*, Vol. 29, No. 2, 2006, pp. 238–246. doi:10.1109/TCAPT.2006.875895

[6] Chen, G., *Nanoscale Energy Transfer and Conversion*, Oxford Univ. Press, New York, 2005.

[7] Jeng, M., Yang, R., and Chen, G., "Monte Carlo Simulation of Thermoelectric Properties in Nanocomposites," *IEEE International Conference on Thermoelectrics*, Inst. of Electrical and Electronics Engineers, Piscataway, NJ, 2005, pp. 21–26.

[8] Pattamatta, A., and Madnia, C. K., "Modeling Heat Transfer in Bi_2Te_3–Sb_2Te_3 Nanostructures," *International Journal of Heat and Mass Transfer*, Vol. 52, Nos. 3–4, 2009, pp. 860–869. doi:10.1016/j.ijheatmasstransfer.2008.09.004

[9] Pattamatta, A., and Madnia, C. K., "Modeling Thermal Transport in Two-Dimensional Nanocomposites," *Bulletin of American Physical Society*, Vol. 51, Nov. 2006, p. 110.

[10] Chung, J. D., and Kaviany, M., "Effects of Phonon Pore Scattering and Pore Randomness on Effective Conductivity of Porous Silicon," *International Journal of Heat and Mass Transfer*, Vol. 43, No. 4, 2000, p. 521. doi:10.1016/S0017-9310(99)00165-9

[11] Joshi, A. A., and Majumdar, A., "Transient Ballistic and Diffusive Phonon Heat Transport in Thin Films," *Journal of Applied Physics*, Vol. 74, No. 1, 1993, pp. 31–39. doi:10.1063/1.354111

[12] Tien, C. L., Majumdar, A., and Gerner, F., *Microscale Energy Transport*, Taylor and Francis, New York, 1997.

[13] Chen, G., "Size and Interface Effects on Thermal Conductivity of Superlattices and Periodic Thin-Film Structures," *Journal of Heat Transfer*, Vol. 119, 1997, pp. 220–229. doi:10.1115/1.2824212

[14] Ziman, J., *Electrons and Phonons*, Oxford Univ. Press, London, 1960.

[15] Zhang, Z., *Nano/Macro Scale Heat Transfer*, McGraw–Hill, New York, 2007.

[16] Swartz, E. T., and Pohl, R. O., "Thermal Boundary Resistance," *Reviews of Modern Physics*, Vol. 61, No. 3, 1989, pp. 605–668. doi:10.1103/RevModPhys.61.605

[17] Fiveland, W. A., "Discrete Ordinate Methods for Radiative Heat Transfer in Isotropically and Anisotropically Scattering Media," *Journal of Heat Transfer*, Vol. 109, No. 3, 1987, pp 809.

[18] Yang, R., and Chen, G., "Thermal Conductivity Modeling of Periodic Two-Dimensional Nanocomposites," *Physical Review B*, Vol. 69, No. 19, 2004, pp. 195316-1–195316-10.

[19] Gropp, W., Lusk, E., and Skjellum, A., *Using MPI Portable Parallel Programming with the Message-Passing Interface*, MIT Press, Cambridge, MA, 1997.

[20] Prasher, R., "Thermal Conductivity of Composites of Aligned Nanoscale and Microscale Wires and Pores," *Journal of Applied Physics*, Vol. 100, No. 3, 2006, pp. 034307-1–034307-9.

[21] Venkatasubramanian, R., "Lattice Thermal Conductivity Reduction and Phonon Localizationlike Behavior in Superlattice Structures," *Physical Review B*, Vol. 61, No. 4, 2000, pp. 3091–3097. doi:10.1103/PhysRevB.61.3091

[22] Narumanchi, S. V. J., Murthy, J. Y., and Amon, C. H., "Comparison of Different Phonon Transport Models for Predicting Heat Conduction In Silicon-on-Insulator Transistors," *Journal of Heat Transfer*, Vol. 127, No. 7, 2005, pp. 713–723. doi:10.1115/1.1924571